

ELECTRONIC SUPPLEMENTARY INFORMATION

Silica-based monoliths functionalized with DTPA for the removal of transition and lanthanide ions from aqueous solutions†

Gioele Ancora^a, Stefano Marchesi^a, Mauro Botta^a, Leonardo Marchese^a, Fabio Carniato^{a*}, and
Chiara Bisio^{a,b*}

^a Dipartimento di Scienze e Innovazione Tecnologica, Università degli Studi del Piemonte Orientale
“Amedeo Avogadro”, Viale Teresa Michel 11, 15121-Alessandria (Italy)

^b CNR-SCITEC Istituto di Scienze e Tecnologie Chimiche “G. Natta”, Via C. Golgi 19, 20133-
Milano (Italy)

*E-mail: chiara.bisio@uniupo.it; fabio.carniato@uniupo.it

*Fax: +39 0131360250; Tel: +39 0131360217, +39 0131360216

1) Figures:

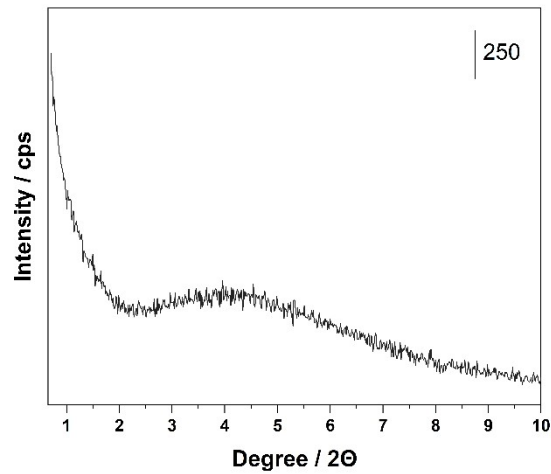


Figure S1. X-ray powder diffractogram of MONO.

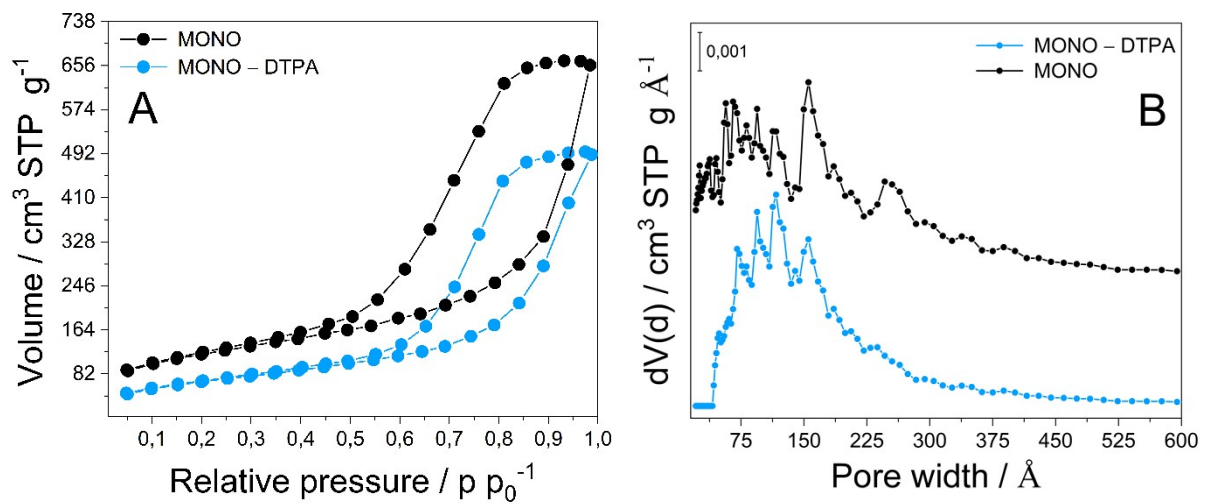


Figure S2: N_2 adsorption/desorption isotherms at 77K (A) and Pore Volume distribution (B) of MONO (-●-) and MONO-DTPA (-●-).

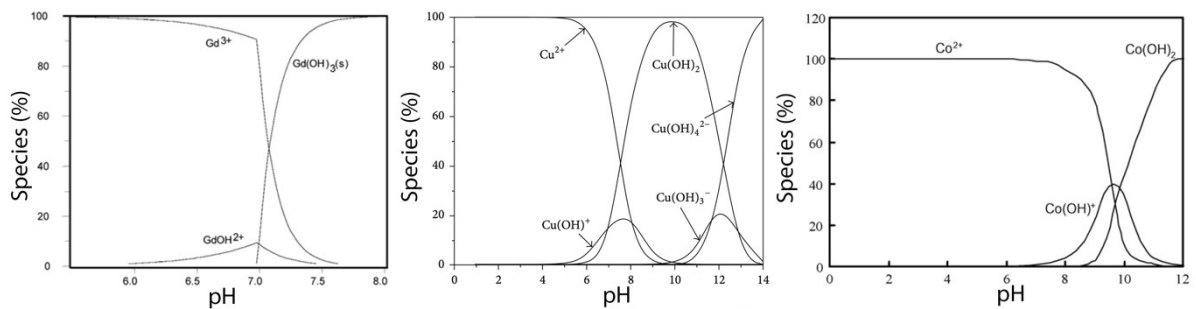


Figure S3. Speciation diagram of Gd^{3+} , Cu^{2+} and Co^{2+} ions as a function of pH.⁵⁸⁻⁶⁰

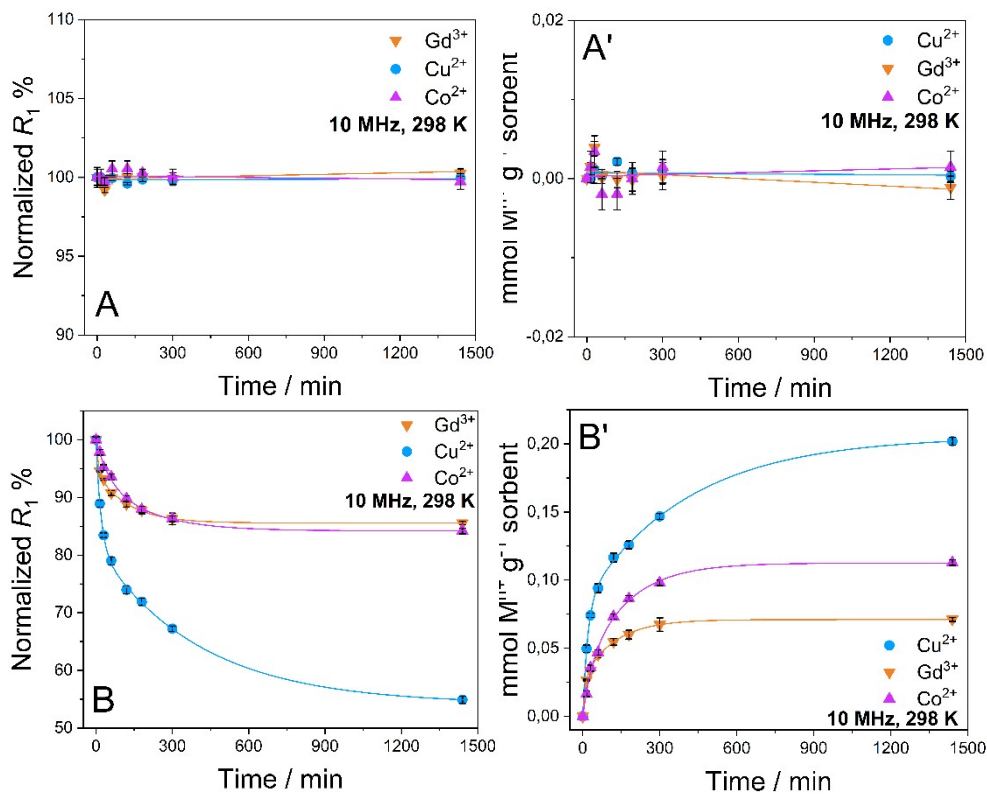


Figure S4. A, B) R_1 percentage decrease overtime; A') amounts of Cu^{2+} , Co^{2+} and Gd^{3+} in mmol of captured metal per g of MONO overtime; B') amounts of Cu^{2+} , Co^{2+} and Gd^{3+} in mmol of captured metal per g of MONO-APTS overtime; (the points represent the mean value and the error bars indicate the standard deviation; $n = 3$).

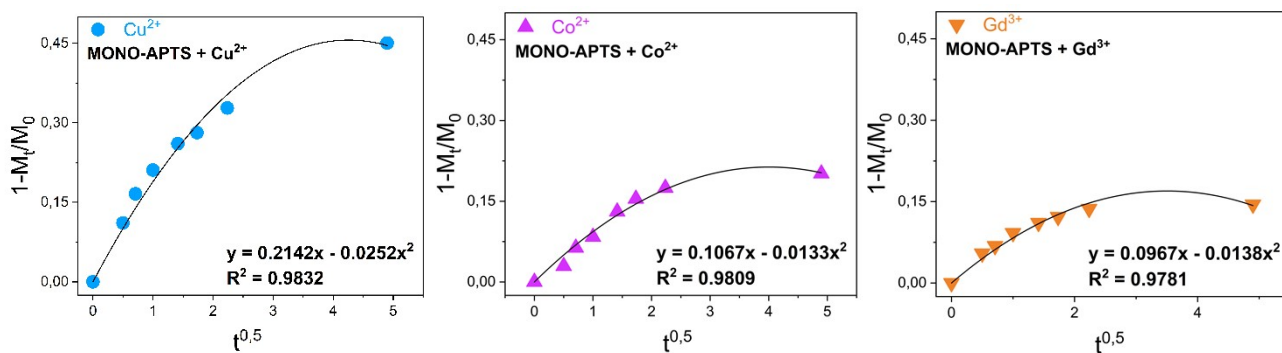


Figure S5. Kinetic analysis of the uptake data for MONO-APTS sample.

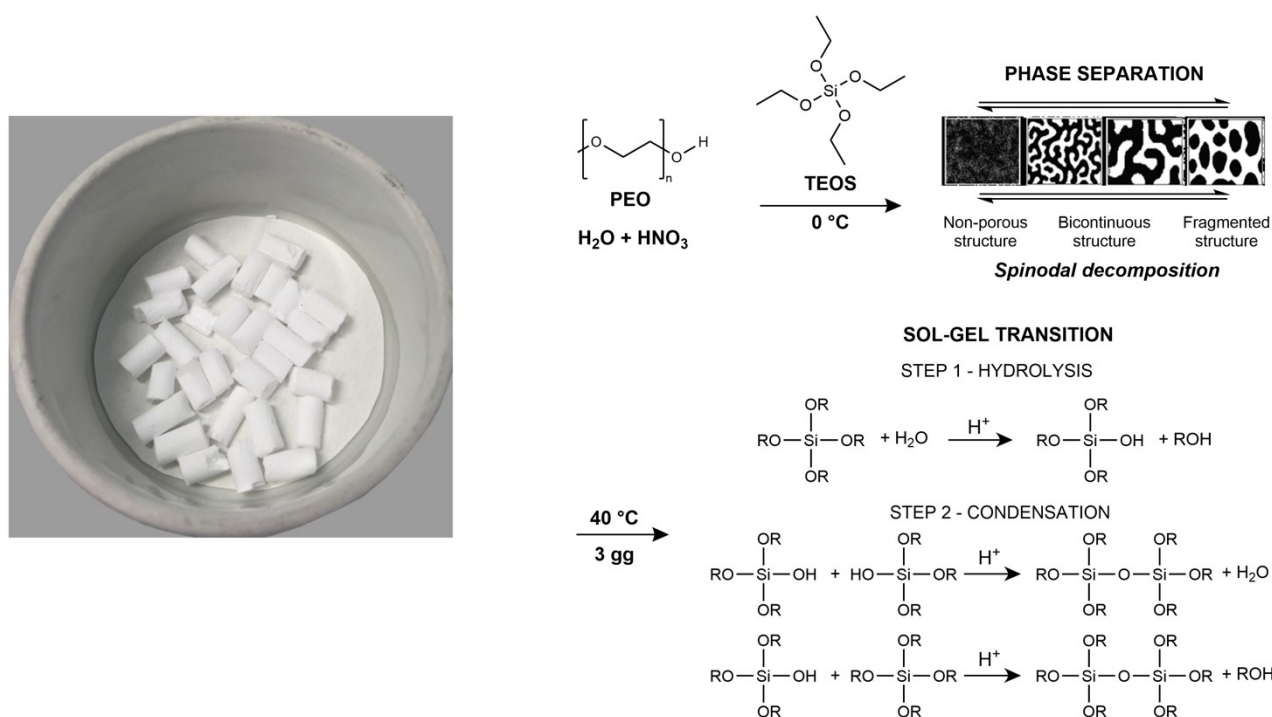


Figure S6. Digital image (left) and synthesis mechanism of MONO (right).

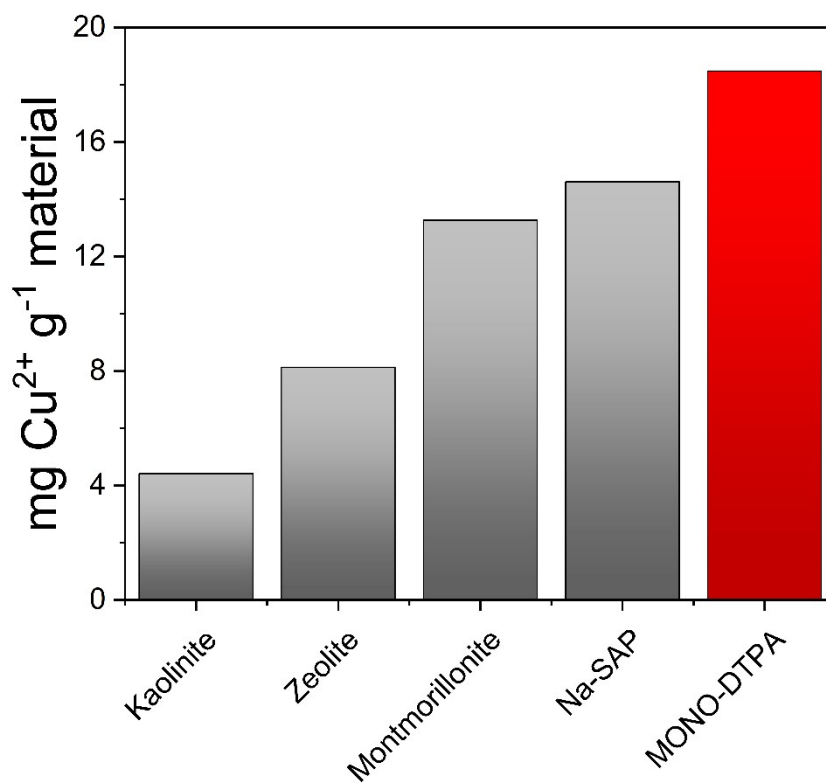


Figure S7. Maximum adsorption capacities of Cu²⁺ ions of MONO-DTPA, Kaolinite clay,⁶⁵ Zeolite,⁶⁶ Montmorillonite clay,⁶⁷ sodium exchanged saponite clay (Na-SAP).⁴⁷

Tables:

Sample	C [%]	N [%]	H [%]	[APTS] (mmol/g)	[DTPA] (mmol/g)
MONO	0.157 ± 0.029	-	1.297 ± 0.053	-	-
MONO-APTS	4.832 ± 0.041	1.894 ± 0.018	1.571 ± 0.078	1.35 ± 0.02	-
MONO-DTPA	9.312 ± 0.028	3.171 ± 0.010	2.226 ± 0.034	-	0.31 ± 0.01

Table S1. Average weight percentages (%) of carbon, nitrogen and hydrogen, and concentration (mmol/g) of APTS and DTPA obtained by CHN analysis on MONO, MONO-APTS and MONO-DTPA; (standard deviations were calculated from a triplicate set of analyses).

Sample	Specific Surface Area (SSA) [m ² /g]	Total Pore Volume [cm ³ /g]	Mesopore Volume [cm ³ /g]	Macropore Volume [cm ³ /g]	Average Pore Diameter [Å]
MONO	430	0.999	0.939	0.060	155
MONO-DTPA	254	0.739	0.711	0.028	117

Table S2. Specific surface area (SSA), volume and average pore diameter values for MONO and MONO-DTPA samples.

Sample	mg M ⁿ⁺ / g sorbent	% Captured M ⁿ⁺ [a]	[APTS] (mmol / g)	Captured [M ⁿ⁺] (mmol / g)
MONO + Gd ³⁺	0.18 ± 0.23	0.0 ± 0.0	-	0.00 ± 0.01
MONO + Cu ²⁺	0.00 ± 0.00	0.1 ± 0.0	-	0.00 ± 0.01
MONO + Co ²⁺	0.09 ± 0.11	0.3 ± 0.3	-	0.00 ± 0.01
MONO-APTS + Gd ³⁺	11.19 ± 0.23	14.5 ± 0.3	1.35 ± 0.03	0.07 ± 0.02
MONO-APTS + Co ²⁺	6.65 ± 0.99	20.1 ± 0.4	1.35 ± 0.03	0.11 ± 0.02
MONO-APTS + Cu ²⁺	12.83 ± 0.18	45.1 ± 0.6	1.35 ± 0.03	0.20 ± 0.03

[a] = in reference to the initial concentration value of each metal solution used (10 mM)

Table S3. Amount of Gd³⁺, Cu²⁺ and Co²⁺ metal ions captured by MONO and MONO-APTS from their respective aqueous solutions after 24h, expressed as mg Mⁿ⁺ / g sorbent, mmol/g and % captured Mⁿ⁺; (standard deviations were calculated from a triplicate set of analyses).

Sample	Gd ³⁺	Co ²⁺	Cu ²⁺
MONO-APTS	$k = 0.0967 \text{ s}^{-1}$ $R^2 = 0.9781$	$K = 0.1067 \text{ s}^{-1}$ $R^2 = 0.9809$	$k = 0.2142 \text{ s}^{-1}$ $R^2 = 0.9832$

Table S4. Kinetic constants (k) and determination coefficient (R^2) obtained by the fitting of the NMR relaxometric data of Fig. S5.

Adsorbent	Uptake capacity (mg/g)	References
MONO-DTPA	18.48	-
Kaolinite	4.42	65
Zeolite	8.13	66
Montmorillonite	13.27	67
Na-SAP	14.61	47

Table S5. Maximum adsorption capacities of Cu^{2+} ions captured by different materials.